

Luminescence from the  ${}^2T_{2g}(H)$  State of Cobalt(II)-Doped  $KCdBr_3$ Robbie G. McDonald,\*<sup>†</sup> Aamer A. Al-Waili, and W. Ewen Smith\*

Department of Pure and Applied Chemistry, Thomas Graham Building, University of Strathclyde, 295 Cathedral Street, Glasgow G1 1XL, United Kingdom

Received January 6, 1994<sup>Ⓢ</sup>

Using argon-ion laser excitation, luminescence has been observed at low-temperature (14 K) in the region between 17 500 and 20 000  $\text{cm}^{-1}$ , for single crystals of cobalt(II)-doped  $KCdBr_3$ . This luminescence is assigned to transitions from the lowest energy component of the  ${}^2T_{2g}(H)$  state,  ${}^2A''$  in the  $C_s$  point symmetry of the cobalt(II) site, into the  ${}^4T_{1g}(F)$  ground state manifold. It gives rise to two broad bands with sharp origins at 20029 and 19127  $\text{cm}^{-1}$  upon which is superimposed considerable vibronic structure. This is believed to be the first example of luminescence detected from the  ${}^2T_{2g}(H)$  state of the cobalt(II) ion. However, as the intensity drops markedly between 14 and 70 K, this transition is not a suitable candidate for the investigation of laser action. Electronic Raman transitions to excited state components of the ground state have been observed, though these are a factor of 50–100 times weaker than the luminescence band origin at 20 029  $\text{cm}^{-1}$ . The energies of the observed electronic Raman transitions were found to correlate with sharp vibronic components of the  ${}^2A''({}^2T_{2g}(H)) \rightarrow {}^4T_{1g}(F)$  transition, which confirmed the ground state spinor component energies to be 262, 500, 902, 1052, and 1118  $\text{cm}^{-1}$ . Finally, the quenching of background emission intensity is indicated by the appearance of “holes” in the observed spectra which are due to absorption into various electronic states of the cobalt(II) ion. This emphasises the importance of crystal quality, the presence of other impurities, and even the role of the host material in determining the optical properties of crystals.

## Introduction

Luminescence from systems involving cobalt(II) ions is comparatively unusual. Many previous studies noting this behavior describe doped semiconductors<sup>1–25</sup> or are relatively

recent,<sup>26–42</sup> a consequence of renewed interest in solid state materials for the development of tunable laser systems.<sup>43–66</sup> Although room-temperature infrared laser action had been demonstrated in the mid 1960's,<sup>67,68</sup> much recent interest has

- \* Authors to whom correspondence should be addressed.  
<sup>†</sup> Present address: CSIRO, Division of Minerals, PO Box 90, Bentley, Western Australia 6102, Australia.  
<sup>Ⓢ</sup> Abstract published in *Advance ACS Abstracts*, March 1, 1995.
- Reynolds, M. L.; Garlick, G. F. J. *Infrared Phys.* **1967**, *7*, 151.
  - Ryskin, A. I.; Khil'ko, G. I. *Opt. Spektrosk.* **1969**, *27*, 183.
  - Busse, W.; Gumlich, H. E.; Maier-Hosch, I. D.; Neumann, E.; Schulz, H.-J. *Proc. Int. Conf. Lumin.*, 1969; Williams, F., Ed.; North-Holland: Amsterdam, 1970; p 66.
  - Busse, W.; Gumlich, H. E.; Neumann, E.; Theis, D. *J. Lumin.* **1971**, *3*, 351.
  - Protsyuk, L. P.; Kh. Rozhko, A. *Ukr. Fiz. Zh.* **1976**, *21*, 1849.
  - Radlinski, A. P. *Phys. Stat. Solidi (b)* **1978**, *86*, 41.
  - Clark, M. G.; Dean, P. J. *Conf. Ser.-Inst. Phys.* **1978**, *42*, 291.
  - Ozeki, M.; Shibatomi, A.; Ohkawa, S. *J. Appl. Phys.* **1979**, *50*, 4823.
  - Bishop, S. G.; Robbins, D. J.; Dean, P. J. *Solid State Commun.* **1979**, *33*, 119.
  - Robbins, D. J.; Dean, P. J.; Giasper, J. L.; Bishop, S. G. *Solid State Commun.* **1980**, *36*, 61.
  - Radlinski, A. P. *J. Lumin.* **1980**, *18–19*, 147.
  - Radlinski, A. P. *J. Phys. C: Solid State Phys.* **1980**, *13*, 2407.
  - Graber, N.; Parsons, R. R.; Schwerdtfeger, C. F.; Czaja, W. *J. Lumin.* **1981**, *22*, 129.
  - Buhmann, D.; Schulz, H.-J.; Thiede, M. *Phys. Rev. B: Condens. Matter* **1981**, *24*, 6221.
  - Renz, R.; Schulz, H.-J. *J. Lumin.* **1981**, *24–25*, 221.
  - Skolnick, M. S.; Dean, P. J.; Tapster, P. R.; Robbins, D. J.; Cockayne, B.; MacEwan, W. R. *J. Lumin.* **1981**, *24–25*, 237; **1981**, *24–25*, 241.
  - Kane, M. J.; Uihlein, C.; Skolnick, M. S.; Dean, P. J.; Hayes, W.; Cockayne, B. *J. Phys. C: Solid State Phys.* **1983**, *16*, 5277.
  - Guillot, G.; Benjeddou, C.; Leyral, P.; Nouailhat, A. *J. Lumin.* **1984**, *31–32*, 439.
  - Schulz, H.-J.; Thiede, M. *Phys. Rev. B* **1987**, *35*, 18.
  - Shirakata, S.; Nishino, T.; Hamakawa, Y.; Kato, T.; Ishida, T. *Jpn. J. Appl. Phys., Part 2* **1987**, *26*, L127.
  - Shirakata, S.; Nishino, T.; Hamakawa, Y. *J. Appl. Phys.* **1988**, *63*, 484.
  - Nishino, T.; Shirakata, S.; Hamakawa, Y. *J. Lumin.* **1988**, *40–41*, 409.
  - Goetz, G.; Schulz, H.-J. *J. Lumin.* **1988**, *40–41*, 415.
  - Goetz, G.; Schulz, H.-J. *Phys. Stat. Solidi (b)* **1992**, *169*, 217.

- Fuchs, F.; Koidl, P. *Solid State Commun.* **1993**, *87*, 791.
- Künzel, W.; Knierim, W.; Dürr, U. *Opt. Commun.* **1991**, *36*, 383.
- Donegan, J. F.; Bergin, F. J.; Imbusch, G. F.; Remeika, J. P. *J. Lumin.* **1984**, *31–32*, 278.
- Babadzhanyan, V. G.; Gabrielyan, V. T.; Kokanyan, E. P.; Kostanyan, R. B.; Sanamyan, T. V. *Zh. Prikl. Spektrosk.* **1985**, *42*, 650.
- Dürr, U.; Brauch, U.; Knierim, W.; Schiller, C. *Springer Ser. Opt. Sci.* **1985**, *47*, 20.
- Suzuki, Y.; Sibley, W. A.; El Bayoumi, O. H.; Roberts, T. M.; Bendow, B. *Phys. Rev. B: Condens. Matter* **1987**, *35*, 4472.
- Lockwood, D. J.; Labbé, H. J. *Proc. SPIE Int. Soc. Opt. Eng.* **1987**, *813*, 129.
- Rowell, N. L.; Lockwood, D. J. *Proc. Electrochem. Soc.* **1988**, *88–24*, 25.
- Rowell, N. L.; Lockwood, D. J. *Infrared Phys.* **1989**, *29*, 385.
- Rowell, N. L.; Lockwood, D. J. *J. Electrochem. Soc.* **1989**, *136*, 3536.
- Strek, W.; Deren, P.; Jezowska-Trzebiatowska, B. *Excited States Transition Elem. Proc. Int. Sch. 1st, 1988*; Jezowska-Trzebiatowska, B., Legendziewicz, J., Streck, W., Eds.; World Sci.: Singapore, 1989; p 490.
- Maana, H.; Moncorgé, R. *Opt. Quantum Electron.* **1990**, *QE-22*, S219.
- Maana, H.; Moncorgé, R. *J. Phys. IV* **1991**, *1*, C7–331.
- Abritta, T.; Blak, F. H. *J. Lumin.* **1991**, *48–49*, 558.
- Sosman, L. P.; Abritta, T. *Solid State Commun.* **1992**, *82*, 801.
- Orera, V. M.; Merino, R.; Cases, R.; Alcalá, R. *J. Phys.: Condens. Matter* **1993**, *5*, 3717.
- Kuleshov, N.; Mikhailov, V. P.; Scherbitsky, V. G.; Prokoshin, P. V.; Yumashov, K. V. *J. Lumin.* **1993**, *55*, 265.
- Deren, P.; Streck, W.; Oetliker, U.; Güdel, H. U. *Phys. Stat. Solidi (b)* **1994**, *182*, 241.
- Mooradian, A. *Rep. Prog. Phys.* **1979**, *42*, 1533.
- Danielmeyer, H. G. *Proc. Int. Conf. Lasers* **1979**, 660.
- Carrigan, B. *Infrared upconversion*; May 1964 Report, 1980. From: *Gov. Rep. Announce. Index (U. S.)* **1980**, *80*, 3796.
- Bhawalkar, D. D.; Nundy, U. *Proc. Symp. Infrared Technol. Instrum.* **1980**, 114.
- Guenther, B. D.; Buser, R. G. *IEEE J. Quantum Electron.* **1982**, *QE-18*, 1179.
- Pine, A. S. *Philos. Trans., R. Soc. London, Ser. A* **1982**, *307*, 469.
- Moulton, P. F. *Laser Focus Fibreopt. Technol.* **1983**, *19*, 83.
- Welling, H. *NATO Adv. Sci. Inst. Ser., Ser. B* **1983**, *95*, 189.
- Moulton, P. F. *Mater. Res. Soc. Symp. Proc.* **1984**, *24*, 393.

centered upon the material, Co<sup>2+</sup>-doped MgF<sub>2</sub>, in the region 1.75–2.5 μm.<sup>69–90</sup> After several years of development, a flash-lamp pumped laser based upon this material is now being used

- (52) Dürr, U. *Solid-state laser materials*; Ger. Offen. DE Patent 3,421,751; 12 Dec 1985, 11 pp.
- (53) *Tunable Lasers, Topics in Applied Physics*, Mollenauer, L. F., White, J. C., Eds.; Springer-Verlag: Berlin, Fed. Rep. Ger., 1987; Vol. 59.
- (54) Imbusch, G. F.; Donegan, J. F.; Bergin, F. J. *Ettore Majorana Int. Sci. Ser.: Phys. Sci.* **1987**, 30, 165.
- (55) Hanna, D. C. *Proc. SPIE-Int. Soc. Opt. Eng.* **1987**, 701, 100.
- (56) Henderson, B.; Imbusch, G. F. *Contemp. Phys.* **1988**, 29, 235.
- (57) Penzkofer, A. *Prog. Quantum Electron.* **1988**, 12, 291.
- (58) Barnes, N. P.; Byvik, C. E. *Proc. SPIE-Int. Soc. Opt. Eng.* **1988**, 889, 92.
- (59) Brenier, A.; Garapan, C.; Madej, C.; Moine, B.; Moncorgé, R.; Monteil, A.; Pedrini, C.; Boulon, G. *Proc. SPIE-Int. Soc. Opt. Eng.* **1990**, 1341, 292.
- (60) Henderson, B.; Yamaga, M.; O'Donnel, K. P. *Opt. Quantum Electron.* **1990**, QE-22, S167.
- (61) Payne, S. A.; Albrecht, G. F. *Solid State Lasers*. In *Encyclopedia of Lasers and Optical Technology*; Meyers, R. A., Ed.; Academic Press Inc.: San Diego, CA, 1991; p 603.
- (62) Aubert, J. J. *Spectra* **2000** **1991**, 155, 56.
- (63) Huber, G. *Phys. Bl.* **1991**, 47, 365, 411.
- (64) Boulon, G. *J. Chim. Phys. Phys.-Chim. Biol.* **1991**, 88, 2299.
- (65) *Tunable Solid State Lasers* [Proceedings of the First International Conference, La Jolla, CA, June 13–15, 1984]; Springer Ser. Opt. Sci.; Hammerling, P., Budgor, A. B., Pinto, A., Eds.; Springer-Verlag: Berlin, Fed. Rep. Ger., 1985; Vol. 47; *Tunable Solid State Lasers for Remote Optical Sensing* [Proceedings of the NASA Conference, Stanford Univ., Stanford, CA, Oct 1–3, 1984]; Springer Ser. Opt. Sci.; Byer, R. L., Gustafson, E. K., Trebino, R., Eds.; Springer-Verlag: Berlin, Fed. Rep. Ger., 1985; Vol. 51. *High Power and Solid State Lasers* (Jan 23–24, 1986, Los Angeles, CA) *Proc. SPIE-Int. Soc. Opt. Eng.* **1987**, 622; Simmons, W. W., Ed.; SPIE-The International Society for Optical Engineering: Bellingham, WA, 1986. *New Slab and Solid State Laser Technology*; (Jan 15–16, 1987, Los Angeles, CA); *Proc. SPIE-Int. Soc. Opt. Eng.* **1987**, 736; Guch, S., Jr., Eggleston, J., Eds.; SPIE-The International Society for Optical Engineering: Bellingham, WA, 1987. *Solid State Lasers* (Jan 15–17, 1990, Los Angeles, CA) *Proc. SPIE-Int. Soc. Opt. Eng.* **1990**, 1223; Dube, G., Ed.; SPIE-The International Society for Optical Engineering: Bellingham, WA, 1990. *Solid State Lasers II* (Jan 24–25, 1991, Los Angeles, CA); *Proc. SPIE-Int. Soc. Opt. Eng.* **1991**, 1420; Dube, G., Ed.; SPIE-The International Society for Optical Engineering: Bellingham, WA, 1991. *Solid State Lasers III* (Jan 20–22, 1992, Los Angeles, CA); *Proc. SPIE-Int. Soc. Opt. Eng.* **1992**, 1627; Quarles, G. J., Ed.; SPIE-The International Society for Optical Engineering: Bellingham, WA, 1992.
- (66) *New materials for advanced solid state lasers* (Symposium held Nov 29–Dec 1, 1993, Boston, MA); Chai, B. H. T., Payne, S. A., Fan, T. Y., Cassanho, A., Allik, T. H., Eds.; Mater. Res. Soc.: Pittsburgh, PA, 1994.
- (67) Johnson, L. F.; Guggenheim, H. J.; Thomas, R. A. *Phys. Rev.* **1966**, 149, 179.
- (68) *Divalent metal doped fluorides as optical maser material*; Dietz, R. E., Guggenheim, H. J., Johnson, L. F. U.S. Patent 3,381,240; April 30, 1968, 5 pp.
- (69) Moulton, P. F.; Mooradian, A. *Solid State Res. Rep. MIT* **1978**, 1, 20.
- (70) Moulton, P. F.; Mooradian, A. *Appl. Phys. Lett.* **1979**, 35, 838.
- (71) Moulton, P. F.; Mooradian, A. *Springer Ser. Opt. Sci.* **1979**, 21, 584.
- (72) Moulton, P. F.; Mooradian, A. *Guoji Jiguanghui Yiweng* **1980**, 437.
- (73) Moulton, P. F. *Proc. Int. Conf. Lasers* **1981**, 359.
- (74) Moulton, P. F. *IEEE J. Quantum Electron.* **1982**, QE-18, 1185.
- (75) Johnson, B. C.; Moulton, P. F.; Mooradian, A. *Opt. Lett.* **1984**, 9, 116.
- (76) Johnson, B. C.; Rosenbluh, M.; Moulton, P. F.; Mooradian, A. *Springer Ser. Chem. Phys.* **1984**, 38, 35.
- (77) Moulton, P. F. *IEEE J. Quantum Electron.* **1985**, QE-21, 1582.
- (78) Loeveld, S.; Moulton, P. F.; Killinger, D. K.; Menyuk, N. *IEEE J. Quantum Electron.* **1985**, QE-21, 202.
- (79) Moulton, P. F. *Springer Ser. Opt. Sci.* **1985**, 47, 4.
- (80) Fox, A. M.; Maciel, A. C.; Ryan, J. F. *Opt. Commun.* **1986**, 59, 142.
- (81) Dürr, U.; Brauch, U. *Springer Ser. Opt. Sci.* **1986**, 52, 151.
- (82) Maciel, A. C.; Maly, P.; Ryan, J. F. *Opt. Commun.* **1987**, 61, 125.
- (83) Welford, D.; Moulton, P. F. *Opt. Lett.* **1988**, 13, 975.
- (84) Harrison, J.; Welford, D.; Moulton, P. F. *IEEE J. Quantum Electron.* **1989**, QE-25, 1708.
- (85) Maciel, A. C.; Maly, P.; Ryan, J. F. *Phys. Rev. A: Gen. Phys.* **1989**, 39, 5455.
- (86) Schneiderova, M.; Maly, P. *Phys. Rev. A: Gen. Phys.* **1990**, 41, 6522.
- (87) Daly, J. G.; Smith, C. A. *Proc. SPIE-Int. Soc. Opt. Eng.* **1992**, 1627, 26.

in both medical and dental applications, and improved eye safety for midinfrared wavelengths makes it a candidate for light detection and ranging (LIDAR) sources and remote sensing instruments designed to operate spacecraft or aircraft.<sup>87</sup> CW infrared laser action has also been demonstrated for Co<sup>2+</sup>-doped KZnF<sub>3</sub>,<sup>26,88,91</sup> while Co<sup>2+</sup>-doped ZnF<sub>2</sub><sup>67,92</sup> and KMgF<sub>3</sub><sup>67,88</sup> have been shown to be potential laser materials.

Normally the parent emitting state of a six coordinate cobalt(II) ion is the lowest energy one, <sup>4</sup>T<sub>2g</sub>, since nonradiative energy transfer mechanisms are often too efficient to allow emission to be observed from higher energy states. However, although the observation of luminescence involving electronic states which are not the closest in energy to the ground state is unusual, it has been noted for Co<sup>2+</sup> ions in various tetrahedral sites.<sup>27,35,40–42,93</sup> In contrast, the Ni<sup>2+</sup> ion doped into a variety of crystals for which the site symmetry is six coordinate exhibits a number of metastable emitting states.<sup>94–100</sup> The authors now wish to describe luminescence involving the cobalt(II) ion in a six coordinate site which arises from the <sup>2</sup>T<sub>2g</sub>(H) state of Co<sup>2+</sup>-doped KCdBr<sub>3</sub> single crystals.

### Experimental Section

Crystals of cobalt(II)-doped KCdBr<sub>3</sub> were produced using KBr, CdBr<sub>2</sub>·4H<sub>2</sub>O, and CoBr<sub>2</sub>·nH<sub>2</sub>O as starting materials. Initially, a 1:1 saturated solution of KBr and CdBr<sub>2</sub>·4H<sub>2</sub>O was heated to remove most of the water and dried overnight at 120 °C. The resultant powder was melted under vacuum in a silica tube to remove residual water, producing crystals of KCdBr<sub>3</sub>. These crystals were ground, a ~3% molar ratio of anhydrous CoBr<sub>2</sub> was added, and the mixture was sealed in silica ampules under vacuum. Crystals of the doped material were grown in a Bridgman furnace at 750–800 °C and, after removal from the cooled ampules, stored in a desiccator.

The crystal structure of KCdBr<sub>3</sub> belongs to the same space group as KCdCl<sub>3</sub>, D<sub>2h</sub><sup>16</sup> (Pnma) (Z = 4).<sup>101,102</sup> This has been verified by X-ray powder studies,<sup>101</sup> Raman spectroscopy,<sup>103</sup> and absorption spectroscopy.<sup>104</sup> The c crystal axis was identified by poor crystal cleavage in this direction, and with the aid of a polarizing microscope, the crystal faces were determined and polished with the polarization directions parallel to the edges. In the KCdX<sub>3</sub> (X = Cl and Br) systems, the Cd<sup>2+</sup> ion site symmetry is rigorously C<sub>s</sub>. Similarly, the point symmetry of a

- (88) Maana, H.; Guyot, Y.; Moncorgé, R. *Phys. Rev. B: Condens. Matter* **1993**, 48, 3633.
- (89) Rines, D. M.; Rines, G. A.; Welford, D.; Moulton, P. F. *OSA Proc. Adv. Solid-State Lasers*; Chase, L. L., Pinto, A. A., Eds.; Opt. Soc. Am.: Washington, DC; p 161.
- (90) Rines, D. M.; Moulton, P. F.; Welford, D.; Rines, G. A. *Opt. Lett.* **1994**, 19, 628.
- (91) German, K. R.; Dürr, U.; Künzel, W. *Opt. Lett.* **1986**, 11, 12.
- (92) Johnson, L. F.; Dietz, R. E.; Guggenheim, H. J. *Appl. Phys. Lett.* **1964**, 5, 21.
- (93) Ferguson, J.; Wood, D. L.; Van Uitert, L. G. *J. Chem. Phys.* **1961**, 51, 2904.
- (94) Vehse, W. E.; Lee, K. H.; Yun, S. I.; Sibley, W. A. *J. Lumin.* **1975**, 10, 149.
- (95) Iverson, M. V.; Sibley, W. A. *J. Lumin.* **1979**, 20, 311.
- (96) Talapatra, D.; Mukherjee, R. K. *Ind. J. Phys.* **1984**, 58A, 205.
- (97) Reber, C.; Güdel, H. U. *Inorg. Chem.* **1986**, 25, 1196.
- (98) Auzel, F.; Breteau, J. M. *J. Phys. Colloq.* **1987**, C7, C7–451.
- (99) May, P. S.; Güdel, H. U. *Chem. Phys. Lett.* **1989**, 164, 612.
- (100) May, P. S.; Güdel, H. U. *Chem. Phys. Lett.* **1990**, 175, 488.
- (101) Seifert, H. J.; Theil, G.; Schmitt, R. *Proc. VI Internat. Conf. Thermal Anal.* (Bayreuth, 1980); Vol. 2, p 81.
- (102) Ledésert, M.; Monier, J. C. *Z. Krist.* **1983**, 165, 199.
- (103) Kuok, M. H.; Tang, S. H. *Phys. Stat. Solidi (b)* **1988**, 147, K195.
- (104) McDonald, R. G.; Al-Waili, A. A.; Smith, W. E. *Chem. Phys.* **1993**, 158, 459.
- (105) Kustov, E. F.; Furiskov, M. A.; Baranov, M. N. *Tr. Mosk. Energ. Inst.* **1972**, No. 143, 70.

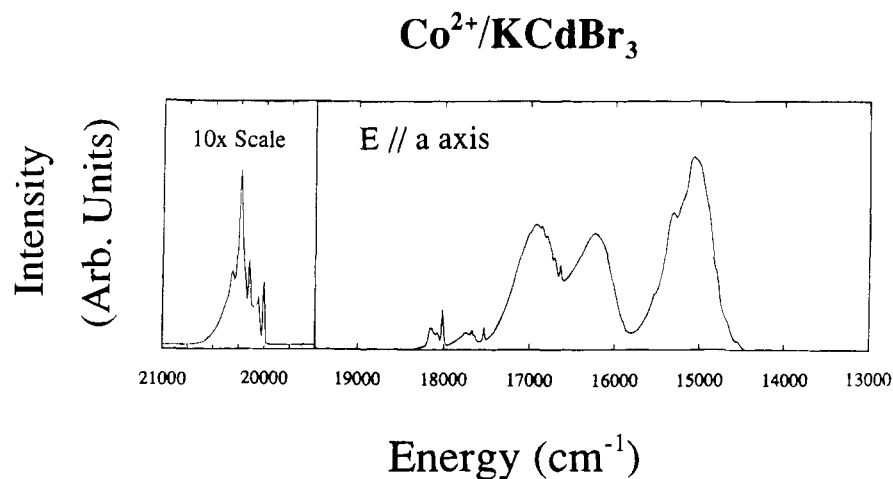


**Figure 1.** Low-temperature (14 K) *a*-polarized absorption spectrum for 2%  $\text{Co}^{2+}$ -doped  $\text{KCdBr}_3$ .<sup>104</sup> The region containing the  ${}^4A''({}^4T_{1g}(F)) \rightarrow {}^2T_{2g}(H)$  transitions has been expanded for clarity.

dopant  $\text{Co}^{2+}$  ion is  $C_s$ , as it has been shown that the polarization properties of the electronic transitions cannot be accounted for in a point group of higher symmetry.<sup>104</sup>

The Raman and luminescence spectra were measured using a Cary 81 spectrophotometer fitted with an S20 photocathode and either the 488.0, 476.5, or 457.9 nm lines of a Spectra-Physics 2020 argon-ion laser excitation source with typical output power of 100 mW. Single crystals of  $\text{Co}^{2+}/\text{KCdBr}_3$  were mounted on a copper block attached to a cold head and cooled by a Displex closed cycle-refrigeration system to a temperature no lower than 14 K. The Raman and luminescence spectra were obtained up to 70 K using a Displex temperature controller and monitored by a Thor cryogenics sensor. Polarized luminescence was obtained by inserting a polarizer and then a polarization scrambler between the sample and the detector. For the purposes of the following discussion of the measured spectra, the energy units are in  $\text{cm}^{-1}$ , the energy of the laser excitation being denoted by  $\nu_{\text{ex}}$  and the energy of the detected radiation by  $\nu$ . The intensities were not corrected for the wavelength response of the monochromator and photomultiplier and hence cannot be compared when different excitation lines of the argon-ion laser have been used.

## Results and Discussion

**Luminescence in Cobalt(II)-Doped Systems.** Luminescence due to the cobalt(II) ion in six coordinate oxide and halide crystals is normally observed in the region of the  ${}^4T_{2g} \rightarrow {}^4T_{1g}(F)$  transition, between 5000 and 7000  $\text{cm}^{-1}$ .<sup>26-42,56,67,91,92,106,107</sup> Ralph and Townsend<sup>106</sup> reported near-infrared fluorescence for the  $\text{Co}^{2+}/\text{MgO}$  system commencing at 8150  $\text{cm}^{-1}$ , assigning transitions from both the  ${}^4T_{2g}$  and  ${}^2E_g$  states. Sturge<sup>107</sup> has observed broad infrared luminescence for the  $\text{Co}^{2+}$ -doped  $\text{KMgF}_3$  system and has identified sharp zero-phonon lines due to the  ${}^4T_{2g}(\Gamma_6) \rightarrow {}^4T_{1g}(\Gamma_6)$  and  ${}^4T_{2g}(\Gamma_6) \rightarrow {}^4T_{1g}({}^{5/2}\Gamma_8)$  transitions at 6900 and 5950  $\text{cm}^{-1}$ , respectively. Similarly, Künzel *et al.*<sup>26</sup> described the luminescence spectra and assigned the highest energy zero-phonon lines for  $\text{Co}^{2+}$  in  $\text{KZnF}_3$ ,  $\text{K}_2\text{ZnF}_4$ , and  $\text{ZnF}_2$ , these occurring at 6601, 6815, and 6510  $\text{cm}^{-1}$ , respectively. Other systems containing six coordinate cobalt(II) for which luminescence has been noted to occur include  $\text{LiNbO}_3$ <sup>28</sup> and several Zr–Ba–La–Al fluoride glasses.<sup>30</sup>

Luminescence has been observed for several acentric four coordinate cobalt(II)-doped systems. For  $\text{Co}^{2+}$  in  $\text{ZnAl}_2\text{O}_4$ ,

luminescence transitions from the  ${}^2E({}^2G)$  state commencing at 11407 and 15723  $\text{cm}^{-1}$  were assigned to the  ${}^4T_2$  and  ${}^4A_2$  final states, respectively,<sup>93</sup> whereas luminescence at 77 K from the  ${}^4T_1(P)$  state and commencing at 15160  $\text{cm}^{-1}$  has been reported for  $\text{Co}^{2+}$ -doped  $\text{LiGa}_5\text{O}_8$ .<sup>27</sup> More recently, Streck *et al.*<sup>35</sup> demonstrated efficient room-temperature broad-band luminescence in the visible region for the first time, for the  $\text{Co}^{2+}$ -doped  $\text{MgAl}_2\text{O}_4$  spinel. Band maxima were located at 14 550 and 14 931  $\text{cm}^{-1}$ . These bands were both assigned to components of the  ${}^4T_1(P) \rightarrow {}^4A_2$  transition. For cobalt(II)-doped zirconia,<sup>40</sup> this transition occurs at 13 330  $\text{cm}^{-1}$ : a band to lower energy, at 10 420  $\text{cm}^{-1}$ , was assigned to the  ${}^4T_1(P) \rightarrow {}^4T_2$  transition. Similarly, the  $\text{Co}^{2+}$ -doped  $\text{LiGa}_5\text{O}_8$ <sup>27</sup> and  $\text{MgAl}_2\text{O}_4$ <sup>35,41-42</sup> systems also show luminescence bands in the infrared region which have been assigned to transitions between excited states,  ${}^4T_1(P) \rightarrow {}^4T_2$  and  ${}^4T_1(P) \rightarrow {}^4T_1(F)$ . Several other oxide systems containing four coordinate cobalt(II) ions have been found to luminesce in the infrared region, viz.  $\text{LaMgAl}_{11}\text{O}_{19}$ ,<sup>37</sup>  $\text{ZnGa}_2\text{O}_4$ ,<sup>38</sup>  $\text{MgGa}_2\text{O}_4$ ,<sup>39</sup> and  $\text{BaAl}_{12}\text{O}_{19}$ .<sup>105</sup>

**Absorption Spectrum of Cobalt(II)-Doped  $\text{KCdBr}_3$ .** The low-temperature (14 K) absorption spectrum of the 2% mole  $\text{Co}^{2+}/\text{KCdBr}_3$  system has previously been reported<sup>104</sup> and the *a*-polarized spectrum in the visible region is shown in Figure 1. This spectrum was found to be consistent with a  $C_s$  site symmetry for the cobalt(II) dopant ion. The assignments and corresponding excited state energies (up to and including the  ${}^2T_{2g}(H)$  state) are presented in Figure 2. Also given are the energies of the ground state spinor components determined in the present study.

**Luminescence from the  ${}^2T_{2g}(H)$  State.** The unpolarized low-temperature luminescence spectrum of the present system, after excitation by the 488.0 nm argon-ion line, exhibits a series of sharp lines commencing at 20 029  $\text{cm}^{-1}$  (Figure 3). This is the energy assigned to the  ${}^4A''({}^4T_{1g}(F)) \rightarrow {}^2A''({}^2T_{2g}(H))$  transition in the absorption spectrum.<sup>104</sup> That the luminescence observed is predominantly due to transitions from the  ${}^2A''({}^2T_{2g}(H))$  state into the ground state manifold was confirmed using excitation by the 476.5 nm line. A similar luminescence spectrum spanning the same range of photon energies was measured (Figure 3), with the first intense zero-phonon transition again being detected at 20 029  $\text{cm}^{-1}$ .

In contrast with the above observations, no sharp luminescence which can be attributed to the  ${}^2A''({}^2T_{2g}(H))$  state of cobalt(II)-doped  $\text{KCdBr}_3$  was detected when the 457.9 nm line was used as the excitation source (Figure 3). Rather, absorption by components of the  ${}^2T_{2g}(H)$  state, assigned to corresponding

(106) Ralph, J. E.; Townsend, M. G. *J. Chem. Phys.* **1968**, *48*, 149.

(107) Sturge, M. D. *Phys. Rev. B*, **1973**, *8*, 6.

|                          |       |                                |   |                                |
|--------------------------|-------|--------------------------------|---|--------------------------------|
| ${}^2T_{2g}(H)$          | ..... | {                              | $\frac{{}^2B_1({}^2A')}{\text{-----}}$  | 20344                          |
|                          |       |                                | $\frac{{}^2A_1({}^2A')}{\text{-----}}$  | 20272                          |
|                          |       |                                | $\frac{{}^2B_2({}^2A'')}{\text{-----}}$ | 20029                          |
| ${}^2A_{1g}(G)$          | ..... |                                | $\frac{{}^2A_1({}^2A')}{\text{-----}}$  | 18137                          |
| ${}^2T_{1g}(P)$          | ..... | {                              | $\frac{{}^2A_2({}^2A'')}{\text{-----}}$ | 18019                          |
|                          |       |                                | $\frac{{}^2B_2({}^2A'')}{\text{-----}}$ | 17642                          |
|                          |       |                                | $\frac{{}^2B_1({}^2A')}{\text{-----}}$  | 17535                          |
| ${}^4T_{1g}(P)$          | ..... | {                              | $\frac{{}^4B_2({}^4A'')}{\text{-----}}$ | 16860                          |
|                          |       |                                | $\frac{{}^4B_1({}^4A')}{\text{-----}}$  | 16240                          |
|                          |       |                                | $\frac{{}^4A_2({}^4A'')}{\text{-----}}$ | 15080                          |
| ${}^2T_{1g}(G)$          | ..... | {                              | $\frac{{}^2B_1({}^2A')}{\text{-----}}$  | 16330                          |
|                          |       |                                | $\frac{{}^2A_2({}^2A'')}{\text{-----}}$ | 16000                          |
|                          |       |                                | $\frac{{}^2B_2({}^2A'')}{\text{-----}}$ | 15900                          |
| ${}^2T_{2g}(G)$          | ..... | {                              | $\frac{{}^2B_1({}^2A')}{\text{-----}}$  | 15510                          |
|                          |       |                                | $\frac{{}^2B_2({}^2A'')}{\text{-----}}$ | 15320                          |
|                          |       |                                | $\frac{{}^2A_1({}^2A')}{\text{-----}}$  |                                |
| ${}^4A_{2g}(F)$          | ..... |                                | $\frac{{}^4A_2({}^4A'')}{\text{-----}}$ | 10800                          |
| ${}^4T_{2g}(F)$          | ..... | {                              | $\frac{{}^4A_1({}^4A')}{\text{-----}}$  | 5700                           |
|                          |       |                                | $\frac{{}^4B_1({}^4A')}{\text{-----}}$  | 5350                           |
|                          |       |                                | $\frac{{}^4B_2({}^4A'')}{\text{-----}}$ | 5200                           |
| ${}^4T_{1g}(F)$          | ..... | {                              | $\frac{{}^4A_2({}^4A'')}{\text{-----}}$ | 1118                           |
|                          |       |                                | $\frac{{}^4B_1({}^4A')}{\text{-----}}$  | 1052                           |
|                          |       |                                | $\frac{{}^4B_2({}^4A'')}{\text{-----}}$ | 902                            |
|                          |       |                                | $\frac{{}^4B_2({}^4A'')}{\text{-----}}$ | 500                            |
|                          |       |                                | $\frac{{}^4B_2({}^4A'')}{\text{-----}}$ | 262                            |
|                          |       |                                | $\frac{{}^4B_2({}^4A'')}{\text{-----}}$ | 0                              |
| Parent symmetry<br>$O_h$ |       | Site symmetry<br>$C_{2v}(C_s)$ | Spin-orbit<br>Coupling                  | Energy<br>( $\text{cm}^{-1}$ ) |

**Figure 2.** Schematic energy level diagram and energy assignments for the observed transitions of the  $\text{Co}^{2+}/\text{KCdBr}_3$  system.<sup>104</sup> The energies for the ground state spinor states determined in the present study are also given. The luminescing  ${}^2A''({}^2T_{2g}(H))$  state of the present study is indicated by a dotted line.

features shown in the expanded region of the spectrum in Figure 1, was observed to be superimposed onto the broad emission background. This suggests either that the 457.9 nm excitation line misses pumping the  ${}^2A''({}^2T_{2g}(H))$  state or a cross-relaxation decay process whereby energy is transferred to a neighboring host site. Although the argon-ion 457.9 nm line is also of

sufficient energy to excite the  ${}^2A''({}^2T_{2g}(H))$  state of the related cobalt(II)-doped  $\text{KCdCl}_3$  system,<sup>104</sup> no luminescence attributable to this state could be detected.

(i)  **${}^4T_{1g}(F)$  Ground State Splitting.** The splitting of the parent  ${}^4T_{1g}(F)$  ground state of six coordinate cobalt(II) halide and doped halide crystals has normally been investigated using

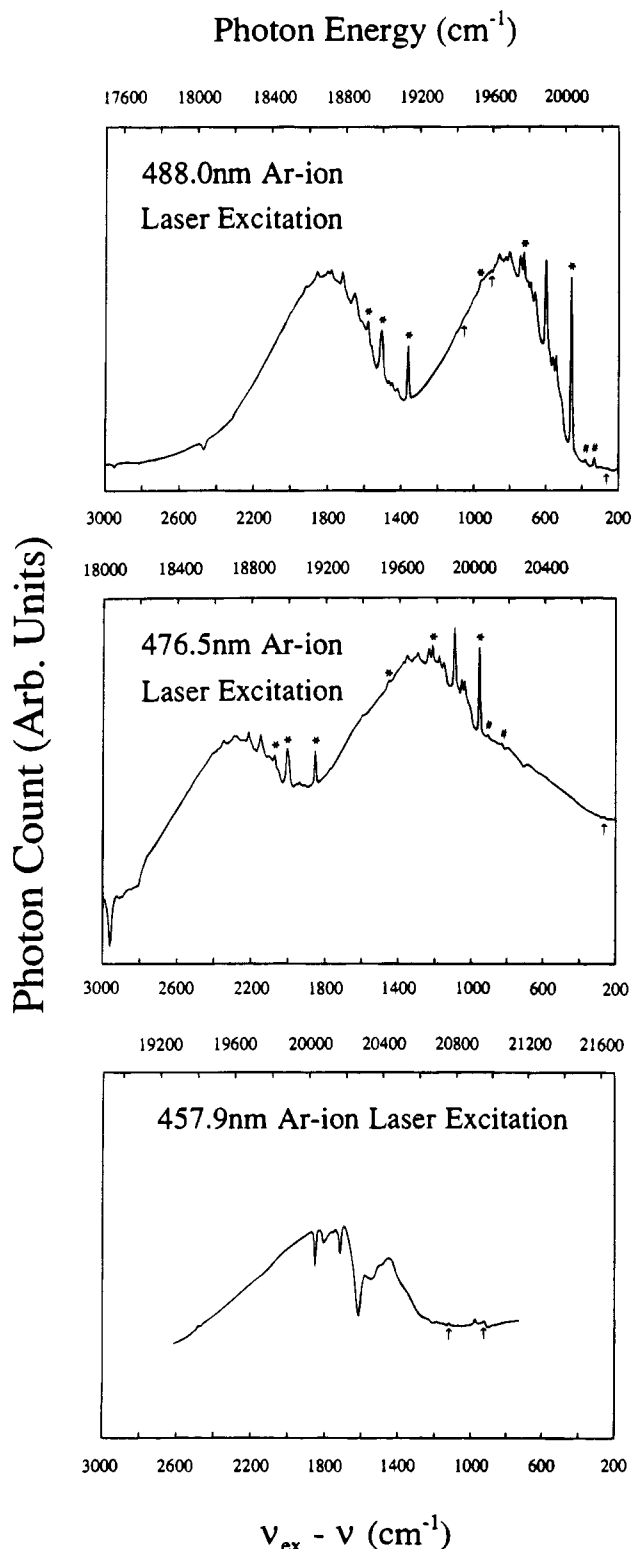


**Figure 3.** Low-temperature (14 K) unpolarized luminescence/Raman spectrum for an arbitrary single crystal face of 2%  $\text{Co}^{2+}$ -doped  $\text{KCdBr}_3$  due to excitation by the 488.0, 476.5, and 457.9 nm argon-ion laser lines. The ground state electronic Raman transitions are indicated by arrows, the zero-phonon single-ion luminescence transitions by stars, and the ion-pair luminescence transitions by cross hatches.

**Raman and infrared spectroscopy.**<sup>108–114</sup> For crystals of cobalt(II)-doped  $\text{KCdBr}_3$  several weak electronic Raman transitions

(108) Jones, G. D.; Kuok, M. H. *J. Phys. C: Solid State Phys.* **1979**, *12*, 715.

(109) Christie, J. C.; Johnstone, I. W.; Jones, G. D.; Zdansky, K. *Phys. Rev. B* **1975**, *12*, 4656.

(110) Johnstone, I. W.; Jones, G. D. *Phys. Rev. B* **1977**, *15*, 1297.

were detected. These appear most clearly in the polarized luminescence spectra shown in Figure 4. However, in contrast with previous investigations, the present study is unusual in that the energies of the  ${}^4\text{T}_{1g}(\text{F})$  state components were confirmed by sharp luminescence transitions originating in the  ${}^2\text{A}''({}^2\text{T}_{2g}(\text{H}))$  state (see below). This compares with the cobalt(II)-doped  $\text{MgF}_2$  system for which the ground state splitting was determined solely from the observation of sharp luminescence transitions from the lowest level of the  ${}^4\text{T}_{2g}$  state.<sup>92</sup>

Two distinct band envelopes, which have sharp intense origins at 20 029 and 19 127  $\text{cm}^{-1}$ , were observed in the low-temperature luminescence spectrum of the  $\text{Co}^{2+}/\text{KCdBr}_3$  crystals (Figures 3 and 4). The separation of these origins suggests that the weak peak with a  $(\nu_{\text{ex}} - \nu)$  energy of  $902 \pm 2 \text{ cm}^{-1}$  is due to a ground state electronic transition. Furthermore, both this and the peak with a  $(\nu_{\text{ex}} - \nu)$  energy of  $1052 \pm 2 \text{ cm}^{-1}$  were just as clearly resolved in the 488.0 nm argon-ion line excited luminescence spectra measured at higher temperatures, 50–70 K (Figure 5). Since the resolution of other features was much reduced, this verifies the independence of the weak peaks from the luminescence mechanism of the  ${}^2\text{A}''({}^2\text{T}_{2g}(\text{H})) \rightarrow {}^4\text{T}_{1g}(\text{F})$  transition. The assignment of the peak at  $1052 \pm 2 \text{ cm}^{-1}$  to an ground state electronic transition was confirmed by the corresponding sharp zero-phonon component at 18 977  $\text{cm}^{-1}$  in the luminescence spectrum. A poorly resolved peak with a  $(\nu_{\text{ex}} - \nu)$  energy of  $1118 \pm 3 \text{ cm}^{-1}$ , is just discernible in the 70 K luminescence spectrum of Figure 5. Assignment of this peak to a ground state electronic transition was established by considering the low-temperature vibronic structure, which corresponds to a number of clear progressions. Neither the peak at  $1118 \pm 3 \text{ cm}^{-1}$  nor the corresponding sharp peak at 18 911  $\text{cm}^{-1}$  can be assigned to progressional components associated with lower energy origins. The full assignment of the vibronic structure, to be discussed below, is given in Table 2.

The absence of fundamental vibrational intervals above 200  $\text{cm}^{-1}$  suggested that the weak peak with a  $(\nu_{\text{ex}} - \nu)$  energy of  $262 \pm 3 \text{ cm}^{-1}$  is also due to an electronic transition, and this was confirmed from both its shape retention up to 70 K (Figure 5) and the position of a corresponding sharp luminescence component at 19 766  $\text{cm}^{-1}$  (Figures 3 and 4). The other ground electronic state was assigned an energy of  $500 \pm 3 \text{ cm}^{-1}$ , from an analysis of the luminescence fine structure which suggested a vibronic progression with origin at 19 529  $\text{cm}^{-1}$ , and associated components with energies of 19 387 and 19 246  $\text{cm}^{-1}$ . That the corresponding electronic Raman peak was not observed is unsurprising since, for the luminescence spectra measured using the 488.0 nm excitation line, overlap occurs with the vibronic structure. Furthermore, low laser output powers were employed,  $\sim 100 \text{ mW}$ . For this reason also, only the electronic Raman transition with  $(\nu_{\text{ex}} - \nu)$  energy of 913  $\text{cm}^{-1}$  was detected in the present study for the related  $\text{Co}^{2+}/\text{KCdCl}_3$  system, in agreement with the finding of Jones and Kuok<sup>108</sup> that this transition is the most intense. Overall, the assignments discussed above are in general agreement with those made for other cobalt(II), halide, and doped halide systems, and the complete ground state spinor assignment is compared with the published data in Table 1.

**(ii) Cobalt(II) Pair Transitions.** Apart from the zero-phonon line of the  ${}^2\text{A}''({}^2\text{T}_{2g}(\text{H})) \rightarrow {}^4\text{A}''({}^4\text{T}_{1g}(\text{F}))$  transition, at 20 029  $\text{cm}^{-1}$ , two significantly weaker bands were resolved at 20 099

(111) Johnstone, I. W.; Jones, G. D.; Lockwood, D. J. *J. Phys. C: Solid State Phys.* **1982**, *15*, 2043.

(112) Jones, G. D.; Tomblin, C. W. *J. Phys. C: Solid State Phys.* **1982**, *15*, 5141.

(113) Tomblin, C. W.; Jones, G. D.; Syme, R. W. G. *J. Phys. C: Solid State Phys.* **1984**, *17*, 4345.

(114) Mischler, G.; Lockwood, D. J.; Zwick, A. *J. Phys. C: Solid State Phys.* **1987**, *20*, 299.

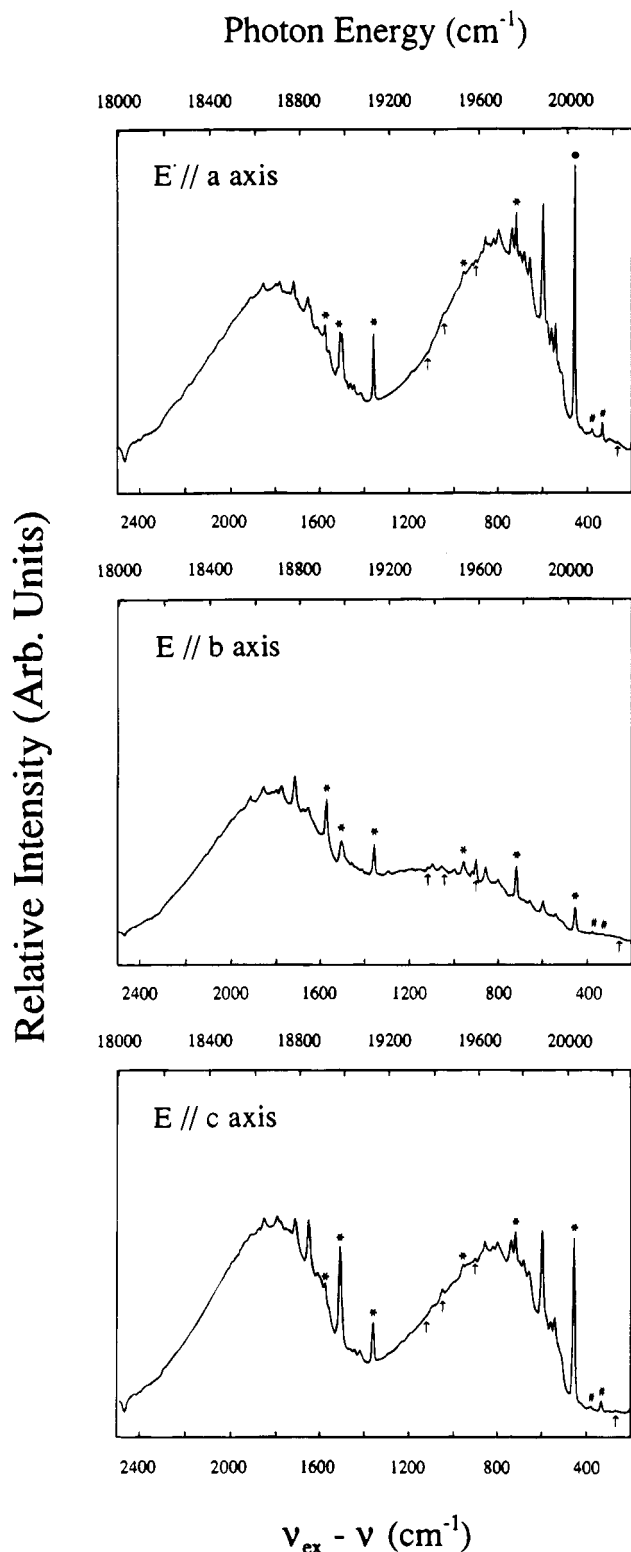


**Figure 4.** Polarized low-temperature (14 K) luminescence/Raman spectra for a single crystal of 2% Co<sup>2+</sup>-doped KCdBr<sub>3</sub> due to excitation by the 488.0 nm argon-ion line. The ground state electronic Raman transitions are indicated by arrows, the zero-phonon single-ion luminescence transitions by stars, and the ion-pair luminescence transitions by cross hatches. The lower scales of each plot refer to the shift from the excitation line, and the upper scales correspond to the energy of the photons detected.

and 20 146 cm<sup>-1</sup> (Figure 3). As these energies do not correspond to those of the <sup>2</sup>T<sub>2g</sub>(H) state components in the absorption spectrum,<sup>104</sup> the peaks are tentatively assigned to the same transition but centered upon one ion of the two possible types of Co<sup>2+</sup> ion pair that can occur in the KCdBr<sub>3</sub> host. The

**Table 1.** Ground State Spinor Energies for Various Six Coordinate Cobalt(II) Halide and Cobalt(II)-Doped Halide Systems (cm<sup>-1</sup>)<sup>a</sup>

| CoCl <sub>2</sub> | CdCl <sub>2</sub> | KCdCl <sub>3</sub> | CsCdCl <sub>3</sub> | MgCl <sub>2</sub>   | CsMgCl <sub>3</sub> | MnCl <sub>2</sub> |
|-------------------|-------------------|--------------------|---------------------|---------------------|---------------------|-------------------|
| 1115              | 1088              | 1188               | 1070                | 1130                | 1379                | 1108              |
| 993               | 948               | 1103               | 947                 | 968                 | 1263                | 972               |
| 962               | 920               | 913                | 873                 | 944                 | 822                 | 938               |
| 545               | 499               | 531 <sup>c</sup>   | 402 <sup>c</sup>    | 543                 | 472                 | 524               |
| 220               | 235               | 251 <sup>c</sup>   | 277 <sup>c</sup>    | 212                 | 233                 | 230               |
| CoBr <sub>2</sub> | CdBr <sub>2</sub> | KCdBr <sub>3</sub> | CsCdBr <sub>3</sub> | CsMgBr <sub>3</sub> |                     |                   |
| 1026              | 995               | 1118               | 1129                | 1231                |                     |                   |
| 941               | 892               | 1052               | 1028                | 1131                |                     |                   |
| 926               | 887               | 902                | 849                 | 837                 |                     |                   |
| 433               | 394               | 500                | 439                 | 448                 |                     |                   |
| 257               | 281               | 262                | 260                 | 247                 |                     |                   |
| CoI <sub>2</sub>  |                   |                    | MgF <sub>2</sub>    |                     |                     |                   |
| 956               |                   |                    | 1398                |                     |                     |                   |
| 895               |                   |                    | 1258                |                     |                     |                   |
| 882               |                   |                    | 1087                |                     |                     |                   |
| 327               |                   |                    | 798                 |                     |                     |                   |
| 220               |                   |                    | 152                 |                     |                     |                   |

<sup>a</sup> Present study, KCdBr<sub>3</sub>; ref 92, MgF<sub>2</sub>; ref 104, c = calculated; ref 108, KCdCl<sub>3</sub>, CsCdCl<sub>3</sub>; ref 109, MnCl<sub>2</sub>; ref 110, CdCl<sub>2</sub>, CdBr<sub>2</sub>, CsMgCl<sub>3</sub>; ref 113, CsCdBr<sub>3</sub>, CsMgBr<sub>3</sub>; ref 114, CoCl<sub>2</sub>, CoBr<sub>2</sub>, CoI<sub>2</sub>.

crystal structure of KCdBr<sub>3</sub>, which is isomorphous with that of KCdCl<sub>3</sub>,<sup>102</sup> contains a double chain of CdBr<sub>6</sub> octahedra, and Co<sup>2+</sup> ion pairs can form within one of the chains or in a staggered arrangement, one cobalt(II) ion in each chain. That the observed peaks are due to luminescence transitions to a component of the ground state is consistent with their decrease in intensity as the temperature is increased to 70 K (Figure 5), which mirrors that of the sharp line at 20 029 cm<sup>-1</sup>. However, their assignment needs to be confirmed by a more detailed study of the effects of varying the cobalt(II) ion concentration upon the luminescence spectrum. Given that the assignment is indeed correct, and assuming that the intensities of the peaks at 20 029 and 20 146 cm<sup>-1</sup> are a linear function of the Co<sup>2+</sup> single ion and ion-pair concentrations, respectively, the ratio of single ions to ion pairs is about 15:1, for the crystals used in this study.

**(iii) Assignment of the Vibronic Structure.** In addition to the zero-phonon lines in the luminescence spectra of Figures 3 and 4, a great deal of associated vibrational fine structure is resolved, and the improved resolution afforded by the polarized spectra (Figure 4) allowed a detailed analysis of this structure, which is presented in Table 2. In common with other systems, the coupling is expected to be predominantly with first-order phonons.<sup>115</sup> The most notable features are vibrational progressions with as many as four components in a mode having an energy of 141(2) cm<sup>-1</sup>, assigned to a totally symmetric Co-Br stretching vibration, for which motion probably involves bridging bromide ions. Bailey and Day<sup>116</sup> also report progressional intervals of 135–140 cm<sup>-1</sup> in the absorption spectra of CoBr<sub>2</sub> and Co<sup>2+</sup>/CdBr<sub>2</sub> crystals, which they assigned in a similar manner. By comparison, for CsCoBr<sub>3</sub> the A<sub>g</sub> phonon was assigned an energy of 168 cm<sup>-1</sup>.<sup>117</sup> As the energies of the Cd-Br symmetric stretching modes of A<sub>g</sub> symmetry in crystals of KCdBr<sub>3</sub> were assigned energies of 151, 176, and 189 cm<sup>-1</sup>,<sup>103</sup> a progressional mode energy of 141(2) cm<sup>-1</sup> would suggest that this vibration is strongly localized on the CoBr<sub>6</sub> chromophore. Such a reduction in energy in this case is not unreasonable

(115) Boudewijn, P. R.; Meetsma, A.; Haas, C. *Physica B+C* **1981**, *106*, 165.

(116) Bailey, A.; Day, P. *Nouv. J. Chim.* **1978**, *1*, 383.

(117) Lehmann, W. P.; Breiting, W.; Weber, R. *J. Phys. C: Solid State Phys.* **1981**, *14*, 4655.

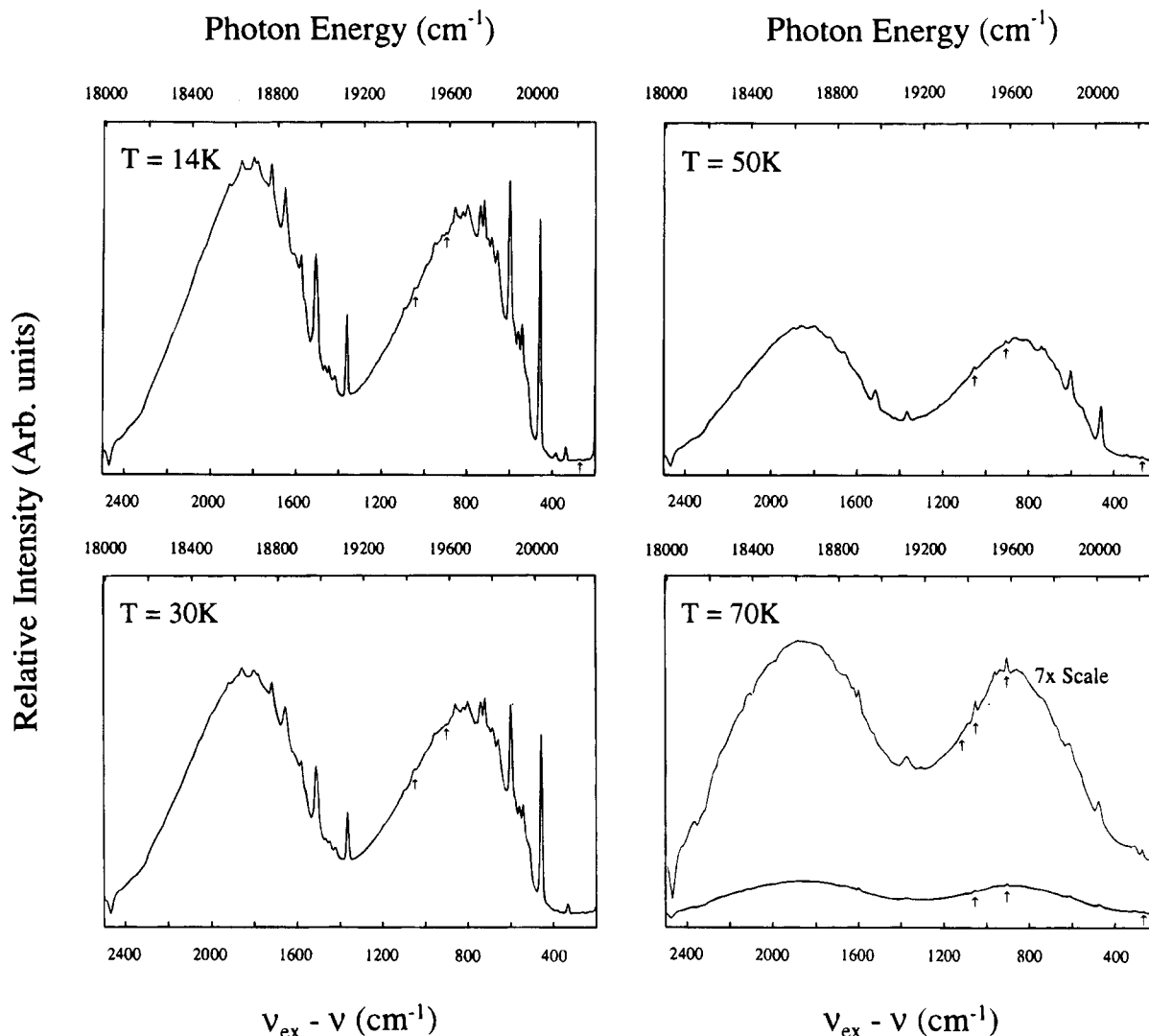


**Figure 5.** Luminescence/Raman spectrum for a single crystal of 2%  $\text{Co}^{2+}$ -doped  $\text{KCdBr}_3$  due to excitation by the 488.0 nm argon-ion line at temperatures of 14, 30, 50, and 70 K. The ground state electronic Raman transitions are indicated by arrows; these are magnified by a factor of 7 in the spectrum measured at 70 K to illustrate their independence from luminescence processes. The lower scales of each plot refer to the shift from the excitation line, and the upper scales correspond to the energy of the photons detected.

because the cobalt(II)–bromide bond lengths are expected to be somewhat longer than in pure systems. However, examination of the Raman spectrum of  $\text{KCdBr}_3$ <sup>103</sup> does reveal a Cd–Br symmetric stretching mode of lower energy, 145  $\text{cm}^{-1}$ , although this was assigned  $B_g$  symmetry.

The patterns observed in the luminescence spectrum suggest that coupling also occurs with modes assigned energies of 57, 85, 103, and 122  $\text{cm}^{-1}$  (Table 2), and this is most apparent in the regions of the spectrum immediately to lower energy than the two sharp origins at 20 029 and 19 127  $\text{cm}^{-1}$ . As there are no Raman active vibrations assigned energies close to 57 and 122  $\text{cm}^{-1}$ ,<sup>103</sup> the associated vibrations are probably of *ungerade* character, consistent with at least some intensity in the luminescence spectrum being induced by a vibronic mechanism. In contrast, vibrations at 86 and 103  $\text{cm}^{-1}$  assigned  $B_g$  and  $A_g$  symmetries, respectively, were detected in the Raman spectrum,<sup>103</sup> though this by no means establishes the modes associated with the vibrational fine structure as being one and the same.

Finally, a second totally symmetric Co–Br stretching vibration, associated with terminal bromide ions, might tentatively be assigned an energy of 162(3)  $\text{cm}^{-1}$ , though coupling with this mode is significantly weaker than that of energy 141(2)  $\text{cm}^{-1}$  (viz. only a single progressional mode was identified).

Again, comparison with the assigned energies of the Cd–Br symmetric stretching modes of  $A_g$  symmetry would suggest that such a vibration is probably strongly localized on the  $\text{CoBr}_6$  chromophore. However, the assignment is also ambiguous since it is not inconceivable that an interval of this magnitude corresponds to a combination of the modes with energies 57 and 103  $\text{cm}^{-1}$ . This conclusion is plausible since, from the above discussion, the latter vibration may have  $A_g$  symmetry.

**(iv) Polarization Properties.** In the  $C_s$  point group of the cobalt(II) dopant site,<sup>104</sup> the ground state electronic components at 500 and 902  $\text{cm}^{-1}$  transform as  ${}^4A'$ , all other states being of  ${}^4A''$  symmetry. The absorption spectra indicate that the  ${}^4A''$ –( ${}^4T_{1g}(F)$ )  $\rightarrow$   ${}^2A''$ ( ${}^2T_{2g}(H)$ ) transition is extremely weak in *b*, and most intense in *a*, polarization. In contrast, the peaks assigned to the  ${}^4A''$ ( ${}^4T_{1g}(F)$ )  $\rightarrow$   ${}^2A'$ ( ${}^2T_{2g}(H)$ ) absorption transitions have significant intensity in all polarizations. The polarized luminescence spectra shown in Figure 4 are also consistent with the former observations, the corresponding  ${}^2A''$ ( ${}^2T_{2g}(H)$ )  $\rightarrow$   ${}^4A''$ –( ${}^4T_{1g}(F)$ ) transition being weakest and most intense, in *b* and *a* polarization, respectively. Examination of the spectra also reveals that the electronic Raman peak at 902  $\text{cm}^{-1}$ , like the corresponding component at 913  $\text{cm}^{-1}$  for the  $\text{Co}^{2+}/\text{KCdCl}_3$  system,<sup>108</sup> is the most intense.

**Table 2.** Assignment of the Vibrational Fine Structure in the Low-Temperature Luminescence Spectrum of Co<sup>2+</sup>-Doped KCdBr<sub>3</sub> (Using 488.0 nm Excitation)<sup>a</sup>

| ( $\nu_{\text{ex}} - \nu$ ) | photon energy | ground state energy | assignment   |
|-----------------------------|---------------|---------------------|--|
| 262                         | 20 225        |                     | ER   |
| 341                         | 20 146        |                     | O <sub>1</sub> (pair)  |
| 388                         | 20 099        |                     | O <sub>1</sub> (pair)  |
| 458                         | 20 029        | 0                   | O <sub>1</sub>   |
| ~515                        | ~20 085       | ~55                 | O <sub>1</sub> + 57  |
| 543                         | 19 943        | 85                  | O <sub>1</sub> + 85  |
| 560                         | 19 926        | 103                 | O <sub>1</sub> + 103   |
| 580                         | 19 906        | 123                 | O <sub>1</sub> + 122   |
| 599                         | 19 887        | 142                 | O <sub>1</sub> + 142   |
| 657                         | 19 829        | 200                 | O <sub>1</sub> + 57 + 142                                      |
| 683                         | 19 803        | 225                 | O <sub>1</sub> + 85 + 140                                      |
| 702                         | 19 784        | 244                 | O <sub>1</sub> + 103 + 141                                     |
| 720                         | 19 766        | 262                 | O <sub>2</sub>   |
| 740                         | 19 747        | 282                 | O <sub>1</sub> + 2 × 141                                       |
| 798                         | 19 689        | 340                 | O <sub>1</sub> + 57 + 2 × 141                                  |
| 803                         | 19 684        | 345                 | O <sub>2</sub> + 85  |
| 822                         | 19 667        | 362                 | O <sub>2</sub> + 103   |
| 841                         | 19 646        | 383                 | O <sub>2</sub> + 121   |
| 860                         | 19 627        | 400                 | O <sub>2</sub> + 140   |
| 902                         | 19 585        |                     | ER   |
| 920                         | 19 567        | 462                 | O <sub>2</sub> + 57 + 142                                      |
| 939                         | 19 548        | 481                 | O <sub>1</sub> + 57 + 3 × 141                                  |
| 958                         | 19 528        | 500                 | O <sub>3</sub>   |
| 1000                        | 19 486        | 542                 | O <sub>2</sub> + 2 × 140                                       |
| 1054                        | 19 432        |                     | ER   |
| 1058                        | 19 428        | 600                 | O <sub>3</sub> + 103   |
| 1099                        | 19 387        | 641                 | O <sub>3</sub> + 142   |
| 1120                        | 19 366        | 662                 | ER/O <sub>3</sub> + 162  |
| 1158                        | 19 328        | 700                 | O <sub>3</sub> + 57 + 142                                      |
| 1198                        | 19 298        | 740                 | O <sub>3</sub> + 103 + 140                                     |
| 1240                        | 19 246        | 782                 | O <sub>3</sub> + 2 × 141                                       |
| 1297                        | 19 189        | 839                 | O <sub>3</sub> + 57 + 2 × 141; O <sub>4</sub> (pair?)          |
| 1360                        | 19 127        | 902                 | O <sub>4</sub>   |
| 1417                        | 19 070        | 960                 | O <sub>4</sub> + 57  |
| 1445                        | 19 042        | 987                 | O <sub>4</sub> + 85  |
| 1464                        | 19 023        | 1006                | O <sub>4</sub> + 103   |
| 1482                        | 19 005        | 1024                | O <sub>4</sub> + 122   |
| 1500                        | 18 987        | 1042                | O <sub>4</sub> + 140   |
| 1510                        | 18 977        | 1052                | O <sub>5</sub>   |
| 1522                        | 18 963        | 1064                | O <sub>4</sub> + 162   |
| 1560                        | 18 927        | 1102                | O <sub>4</sub> + 57 + 142                                      |
| 1576                        | 18 911        | 1118                | O <sub>6</sub>   |
| 1601                        | 18 886        | 1143                | O <sub>5</sub> + 85; O <sub>4</sub> + 103 + 141                |
| 1644                        | 18 843        | 1186                | O <sub>4</sub> + 2 × 142                                       |
| 1653                        | 18 835        | 1194                | O <sub>5</sub> + 142   |
| 1658                        | 18 830        | 1199                | O <sub>6</sub> + 85  |
| 1679                        | 18 809        | 1220                | O <sub>6</sub> + 103   |
| 1702                        | 18 785        | 1244                | O <sub>4</sub> + 57 + 2 × 142; O <sub>6</sub> + 122            |
| 1717                        | 18 770        | 1259                | O <sub>6</sub> + 141   |
| 1742                        | 18 745        | 1284                | O <sub>5</sub> + 85 + 142; O <sub>4</sub> + 103 + 2 × 141      |
| 1777                        | 18 710        | 1319                | O <sub>6</sub> + 57 + 142                                      |
| 1797                        | 18 690        | 1339                | O <sub>5</sub> + 2 × 142                                       |
| 1801                        | 18 696        | 1343                | O <sub>6</sub> + 85 + 140                                      |
| 1858                        | 18 629        | 1400                | O <sub>6</sub> + 2 × 141                                       |
| 1903                        | 18 584        | 1445                | O <sub>5</sub> + 103 + 2 × 142 (?)                             |
| 1917                        | 18 571        | 1458                | O <sub>6</sub> + 57 + 2 × 141                                  |
| 1960                        | 18 528        | 1501                | O <sub>6</sub> + 103 + 2 × 141                                 |
| 1998                        | 18 490        | 1539                | O <sub>6</sub> + 3 × 141                                       |
| 2056                        | 18 432        | 1597                | O <sub>6</sub> + 57 + 3 × 141                                  |
| 2111                        | 18 377        | 1652                | O <sub>6</sub> + 103 + 3 × 141; O <sub>6</sub> + 122 + 3 × 141 |

<sup>a</sup> All energies are in cm<sup>-1</sup>. O<sub>1</sub> to O<sub>6</sub> refer to transitions to ground state electronic origins. ER = Electronic Raman transition.

(v) **Band Shape Analysis.** The clear resolution of two luminescence band envelopes for the Co<sup>2+</sup>/KCdBr<sub>3</sub> system indicates that the electron-phonon coupling constant, or Huang-Rhys factor, is smaller for transitions to the ground state from the <sup>2</sup>T<sub>2g</sub>(H), than the <sup>4</sup>T<sub>2g</sub>, state. This follows since,

normally, the spectra of cobalt(II)-doped systems in the region of <sup>4</sup>T<sub>2g</sub> → <sup>4</sup>T<sub>1g</sub>(F) emission exhibit a single band.<sup>26,31,92,106-107</sup> From the intensity distribution,  $I_n$ , within a totally symmetric vibrational progression, the Huang-Rhys parameter  $S$  can be calculated by

$$I_n/I_0 = S^n/n!$$

where  $n$  is the number of  $a_g$  quanta involved. The intensities of the first three members of the progression of the highest energy <sup>2</sup>A''(<sup>2</sup>T<sub>2g</sub>(H)) → <sup>4</sup>A''(<sup>4</sup>T<sub>1g</sub>(F)) luminescence transition, at 20 029, 19 887, and 19 747 cm<sup>-1</sup>, give a calculated value of 0.55 ± 0.05 for  $S$ . This compares with values for  $S$  of 2.5 ± 0.2 and 5.6 ± 0.5 estimated by Reber and Güdel<sup>92</sup> for the lowest energy <sup>3</sup>T<sub>2g</sub> → <sup>3</sup>A<sub>2g</sub> luminescence transition of nickel(II)-doped CsMgCl<sub>3</sub> and CsMgBr<sub>3</sub> crystals, respectively, and which are expected to be similar for the <sup>4</sup>T<sub>2g</sub> → <sup>4</sup>T<sub>1g</sub>(F) transitions of the corresponding cobalt(II)-doped systems.

(vi) **General Considerations.** The recent focus upon new transition metal doped hosts as potential broad-band tunable lasers has targeted those materials which luminesce at, or near to, room temperature as being most promising for further investigation.<sup>56,61</sup> In this respect, the effect of temperature upon the <sup>2</sup>A''(<sup>2</sup>T<sub>2g</sub>(H)) → <sup>4</sup>T<sub>1g</sub>(F) luminescence was investigated and spectra obtained at temperatures up to 70 K are shown in Figure 5. Clearly, nonradiative decay processes begin to dominate at relatively low-temperatures causing a rapid drop in luminescence intensity and this is consistent with the low energy, 141(2) cm<sup>-1</sup>, of the  $\nu(\text{Co}-\text{Cl})$  stretching vibration expected to participate strongly in these processes.<sup>118</sup> Therefore, the present spin-forbidden luminescence is probably not a suitable candidate for the further investigation of laser action, even if the cobalt(II) concentration was decreased or the quality of the Co<sup>2+</sup>/KCdBr<sub>3</sub> crystals improved by more rigorous control of the growth conditions.

As the energy gap from the <sup>2</sup>A''(<sup>2</sup>T<sub>2g</sub>(H)) state to the next lower <sup>2</sup>A'(<sup>2</sup>A<sub>1g</sub>(G)) state<sup>104</sup>, 1892 cm<sup>-1</sup>, corresponds to more than thirteen quanta of the  $\nu(\text{Co}-\text{Cl})$  stretching vibration, this probably accounts for the observation of luminescence from the <sup>2</sup>A''(<sup>2</sup>T<sub>2g</sub>(H)) state in the first instance, since the break-even point between radiative and non-radiative processes typically occurs when the energy gap can be bridged by about six vibrational quanta.<sup>118</sup> In contrast for the well studied Co<sup>2+</sup>/MgF<sub>2</sub> system, the "effective" energy of such a vibration will be similar to that of the host A<sub>1g</sub> phonon,<sup>119</sup> 410 cm<sup>-1</sup>. Since in the stronger ligand field of the fluoride host the energy gap is expected to be smaller, the transition will involve only three to four vibrational quanta and non-radiative decay from the <sup>2</sup>T<sub>2g</sub>(H) state will dominate.

Finally, in considering the present system as a potential laser material, examination of the emission intensity down to an energy of ~14 000 cm<sup>-1</sup> did not reveal luminescence originating from other metastable states of the cobalt(II) ion. This, however, does not preclude further studies which might detect luminescence from the lowest energy <sup>4</sup>T<sub>2g</sub> → <sup>4</sup>T<sub>1g</sub>(F) transition or search for luminescence transitions between metastable states, e.g. <sup>2</sup>A''-(<sup>2</sup>T<sub>2g</sub>(H)) → <sup>4</sup>A''(<sup>4</sup>T<sub>1g</sub>(P)), as such transitions have been observed for Co<sup>2+</sup> ions in the tetrahedral sites of the LiGa<sub>5</sub>O<sub>8</sub><sup>27</sup> and MgAl<sub>2</sub>O<sub>4</sub> hosts.<sup>35,41-42</sup> Site-selective pumping of various cobalt(II) sites might also be considered in crystals having a range of cobalt(II) concentrations. Studies of this and the above kind

(118) Henderson, B.; Imbusch, G. F. *Optical Spectroscopy of Inorganic Solids*; Clarendon Press: Oxford, England, 1989; Chapter 5.

(119) Porto, S. P. S.; Fleury, P. A.; Damen, T. C. *Phys. Rev.* **1967**, *154*, 522.



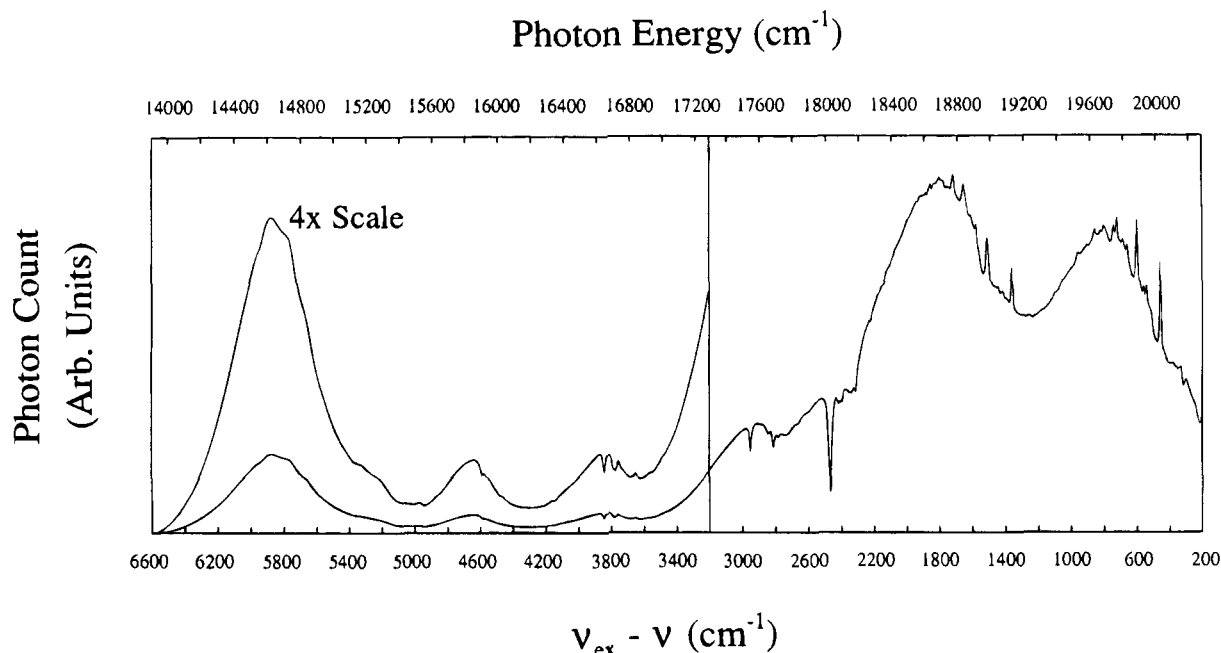


**Figure 6.** Unpolarized low-temperature luminescence (14 K) for a single crystal of 2%  $\text{Co}^{2+}$ -doped  $\text{KCdBr}_3$  due to excitation by the 488.0 nm argon-ion line. This spectrum was measured after "aging" well-polished crystal faces (cf. the corresponding measurement in Figure 3). The region of the spectrum shifted more than  $3500\text{ cm}^{-1}$  from the excitation line is expanded by a factor of 4.

by the present authors were not possible due to equipment limitations, viz. the excitation source, the diffraction grating, and the detector.

#### Host Crystal, Impurity, and Surface Site Luminescence.

The spectrum due to the luminescence from the  ${}^2A''({}^2T_{2g}(\text{H}))$  state is superimposed upon that due to other emission processes. For  $\text{Co}^{2+}$ -doped systems, luminescence due to  $\text{Ni}^{2+}$  impurities has also been identified<sup>92</sup> and may contribute strongly to the background intensity in the present case. In addition, luminescence of the host material is quite likely since bands assigned to emission from  $\text{Br}_2^{2-}$  centers at 3.3, 2.0, and 1.8 eV (i.e. 26 600, 16 100, and 14 500  $\text{cm}^{-1}$ ) have been observed for the related host material  $\text{CsCdBr}_3$ .<sup>120</sup> Finally, the present crystals are slightly hygroscopic and clearer polished crystal surfaces were observed to "cloud" over a period of time. This may produce new sites at which emission occurs.

The competition between absorption and emission processes is an important factor if there is significant overlap between the absorption and luminescence bands, as self-absorption often degrades the performance of transition metal doped crystals as laser materials.<sup>56</sup> For the  $\text{Co}^{2+}/\text{KCdBr}_3$  system self-absorption has only a small effect on the  ${}^2A''({}^2T_{2g}(\text{H})) \rightarrow {}^4T_{1g}(\text{F})$  transition, being apparent on the low-energy tail of the lower energy band envelope (Figures 3 and 6). As part of the self-absorption process, there is, in general, a decrease in the background emission intensity which manifests itself as "holes" due to sharp states of the cobalt(II) ion. The energies of the most prominent "dips" in Figure 6 (at 18 019, 17 642, 17 535, 16 701, 16 644, 16 334,  $\sim 16\,000$ , and 15 897  $\text{cm}^{-1}$ ) correspond to spin-forbidden transitions to components of the  ${}^2A_{1g}(\text{G})$ ,  ${}^2T_{1g}(\text{P})$ , and  ${}^2T_{1g}(\text{G})$  states, which occur in the absorption spectrum (Figure 1). Similar absorption "dips" have been noted in the investigation of the  $\text{Co}^{2+}/\text{MgCl}_2$  system;<sup>121</sup> "holes" due to absorption by components of the  ${}^2A_{1g}(\text{G})$  and  ${}^2T_{1g}(\text{P})$  states have also been observed for the  $\text{Co}^{2+}/\text{KCdCl}_3$  system. The size of the "dips" was found to be dependent upon the position of the laser beam

relative to the crystal surface, the background emission intensity, and the quality of the crystal surface.

A comparison of the background intensity for the plots of Figure 3 suggests a broad underlying emission band centered at  $\sim 20\,200\text{ cm}^{-1}$  in the spectrum obtained using 476.5 nm excitation. This is probably due to a change in the quality of the crystal surface, as the same crystal was used for both measurements. The "aging" of highly polished crystal faces in the atmosphere also caused the absorption "dips" to become more pronounced relative to the  ${}^2A''({}^2T_{2g}(\text{H})) \rightarrow {}^4T_{1g}(\text{F})$  luminescence bands (Figure 6). Presumably, this is due to the effects of surface degradation such as oxidation and water adsorption. Not only can new luminescing species be produced in the near-surface layers of the crystal, but surface degradation will cause diffusion of the incident laser beam, reducing the excitation energy at any one site and increasing the relative efficiency of the absorption process.

The most interesting feature of Figure 6 is the appearance of a broad-band luminescence transition commencing at  $\sim 15\,200\text{ cm}^{-1}$  which seems to show a weakly resolved vibronic progression in a mode of energy  $\sim 100\text{ cm}^{-1}$  and an intensity maximum at  $\sim 14\,600\text{ cm}^{-1}$ . This band cannot be due to a nickel(II) impurity since there is no corresponding absorption band for the analogous  $\text{Ni}^{2+}/\text{KCdBr}_3$  system.<sup>122</sup> Furthermore, it cannot be assigned to a  ${}^4T_{1g}(\text{P}) \rightarrow {}^4T_{1g}(\text{F})$  transition of the cobalt(II) ion. Close examination shows that several of the sharp "dips" mentioned above are superimposed upon broad-band absorptions corresponding to the  ${}^4A''({}^4T_{1g}(\text{F})) \rightarrow {}^4A'$ ,  ${}^4A''({}^4T_{1g}(\text{P}))$  absorption transitions of the  $\text{Co}^{2+}/\text{KCdBr}_3$  system which occur at 16 240 and 16 860  $\text{cm}^{-1}$ , respectively (Figure 1). In addition, luminescence from the lowest energy  ${}^4A''({}^4T_{1g}(\text{P}))$  component, which has a maximum at 15 080  $\text{cm}^{-1}$  in the absorption spectrum (Figure 1), is expected to commence at  $\sim 14\,500\text{ cm}^{-1}$  and have an approximate mirror image symmetry to the absorption band. Further examination of Figure 6 also suggests that since the structure on the observed feature cannot be detected to lower energies than  $\sim 14\,500\text{ cm}^{-1}$ , it appears

(120) Andraud, C.; Pelle, F.; Denis, J. P.; Pilla, O.; Blanzat, B. *J. Phys.: Condens. Matter* **1989**, *1*, 1511.

(121) Wilson, D. R.; Smith, W. E. Unpublished data.

(122) McDonald, R. G.; Christie, P. M.; Smith, W. E. Unpublished data.

likely that the pattern observed can be also be explained by absorption, into the lowest energy  ${}^4A''({}^4T_{1g}(P))$  component. Similarly, deviations in the photon count at 15 200, ~15 300, and 15 511  $\text{cm}^{-1}$  may be due to absorption, by components of the  ${}^2T_{2g}(G)$  state.

The source of the emission intensity upon which is superimposed absorption into the  ${}^4T_{1g}(P)$  manifold could be due to a  $\text{Br}_2^{2-}$  center; the luminescence properties assigned to this species in  $\text{CsCdBr}_3$  correspond to bands centered at 14 500 and 16 100  $\text{cm}^{-1}$ .<sup>118</sup> However, it is not inconceivable that the  ${}^2A''({}^2T_{2g}(H)) \rightarrow {}^4T_{2g}$  excited state luminescence transition is being observed. Examination of the energy level diagram in Figure 2 indicates that this transition would be expected to have maximum absorption at about 14 800  $\text{cm}^{-1}$ . If this were the case it is likely that luminescence from the  ${}^4T_{2g} \rightarrow {}^4T_{1g}(F)$  transition can also be detected.

### Conclusions

The present study of  $\text{Co}^{2+}/\text{KCdBr}_3$  has demonstrated the first example of luminescence originating in the  ${}^2T_{2g}(H)$  state of the

cobalt(II) ion. The vibrational fine structure associated with the  ${}^2A''({}^2T_{2g}(H)) \rightarrow {}^4T_{1g}(F)$  transition has allowed the energies of the ground state spinor components to be determined and for several of these, confirms the observation of the corresponding weak electronic Raman transitions. Furthermore, the observed spectra were found to be dependent upon the energy of the laser excitation line, the state of degradation of the crystal surfaces, and the presence of other luminescing sites within the crystal bulk.

Although the  ${}^2A''({}^2T_{2g}(H)) \rightarrow {}^4T_{1g}(F)$  transition does not appear to be a good candidate for sustaining laser action at room temperature, investigations of the luminescence due to the  ${}^4T_{2g} \rightarrow {}^4T_{1g}(F)$  transition are worth pursuing for both the present system and the analogous cobalt(II)-doped  $\text{KCdCl}_3$  material.

**Acknowledgment.** One of us (R.G.M.) wishes to thank the University of Strathclyde for the support provided by the Research and Development Fund.

IC940011R